RSC Advances

PAPER

View Article Online
View Journal | View Issue

Cite this: *RSC Adv.*, 2017, **7**, 1581

Theoretical and experimental study on the degradation mechanism of atrazine in Fenton oxidation treatment†

Xue Zhao,[a] Chenxi Zhang,[b] Shuguang Wang,*[c] Chao Song[c] and Xiang Li*[d]

Received 17th November 2016
Accepted 17th December 2016

DOI: 10.1039/c6ra26918d

www.rsc.org/advances

The residues of atrazine in surface and ground water will cause harm to human health as they are slowly biodegraded microbiologically. In this work, density functional theory (DFT) and the polarizable continuum model (PCM) were used to investigate the degradation of atrazine in an aqueous medium by Fenton oxidation technology. The results show that H atom abstraction pathways are more probable than both OH radical addition and Cl atom substitution pathways. Moreover, the H atom abstraction from the –CH– of $-CH(CH_3)_2$ group and $-CH_2-$ of $-CH_2CH_3$ group are expected to occur more easily. New dealkylation and alkyl oxidation mechanisms are proposed, in which water can act as a catalyst to reduce the reaction barrier dramatically. The stable intermediates and products: CH_3COCH_3, DEDIA, DIA, DEA, CAFT, CDAT, CDET, CDFT and CFIT, have been identified with LC/MS analysis. This study offers a cost-effective way to probe the degradation mechanism of atrazine in an aqueous medium by Fenton oxidation technology.

Introduction

Triazine is used worldwide to combat grassy and broadleaf weeds in many agricultural crops as well as for non-agricultural purposes, such as soil sterilization and road maintenance.[1] Atrazine (ATZ), with its chemical name 2-chloro-4-ethylamino-6-isopropylamino-*s*-triazine ($C_8H_{14}ClN_5$), is the main representative of the *s*-triazines and has been most widely used in the world in the last several decades.[2–4] It was detected ubiquitously in surface and ground water in many countries. ATZ has been identified as a putative endocrine disruptor and classified as a class C carcinogen.[5–8] The chromosomes of Chinese hamster egg cells will be damaged if they are exposed to 1.08–17.26 μg L^{-1} of ATZ within two days. The widespread use of ATZ has caused concentrations exceeding the limit of surface and ground water throughout Europe and the United States.[9,10] Thus, the commercial use of ATZ has been banned in several countries.[11] However, its presence in surface and ground water continues to last for several years. The search for effective methods to remove ATZ from water is of importance.

Water treatment processes include physical processes,[12,13] biological processes,[14–16] chemical processes,[17,18] catalytic oxidation[19,20] and several advanced oxidation processes (AOPs).

In general, absorption and extraction are cost effective and easy to perform. However, they only transfer the pollutant to another phase, without promoting its degradation to a less harmful species.[21] ATZ is toxic to microorganisms, and the triazine-ring itself is quite resistant to microbial attacks.[22,23] As a result, conventional biological remediation is neither efficient and nor suitable for removing higher concentrations of ATZ from contaminated water rapidly. In the chemical process, AOPs are potentially useful to treat pesticide wastes because they generate powerful oxidizing agents. Several AOPs have been applied to ATZ degradation in the aqueous medium, such as sonolysis,[24,25] electron-beam irradiation,[26] TiO_2-supported UV photolysis,[27,28] O_3/UV,[29,30] UV/H_2O_2,[31,32] O_3/H_2O_2 (ref. 33) and Fenton oxidation technology, which includes Fenton, photo-Fenton, and electro-Fenton.[34–40]

Fenton oxidation technology, which generates hydroxyl radical (OH), is a promising method to treat wastewater containing ATZ. The Fenton system consists of a mixture of ferrous salt (Fe^{2+}) and H_2O_2, namely Fenton's reagent. OH can be produced in the reaction, $H_2O_2 + Fe^{2+} \rightarrow Fe^{3+} + OH^- + OH$. Laat has compared the efficiencies of degradation of ATZ by several AOPs, and found that the photo-Fenton process was more efficient than H_2O_2/UV.[35] Khan have compared the degradation of ATZ by photo-Fenton and photo-Fenton-like oxidation technologies. It is suggested that they are capable of removing ATZ

[a]*College of Chemistry, Chemical Engineering and Materials Science, Shandong Normal University, Jinan 250014, P. R. China*

[b]*Department of Resources and Environment, Binzhou University, Binzhou 256600, P. R. China*

[c]*School of Environmental Science and Engineering, Shandong University, Jinan 250100, P. R. China. E-mail: wsg@sdu.edu.cn*

[d]*Department of Environmental Science & Engineering, Fudan University, Shanghai 200433, P. R. China. E-mail: lixiang@fudan.edu.cn*

† Electronic supplementary information (ESI) available: The dealkylation and alkyl oxidation process of IM11 in aqueous medium by Fenton oxidation technology. See DOI: 10.1039/c6ra26918d

from water efficiently, but this study did not cover the degradation mechanism.[40] Balci has studied the degradation mechanism of ATZ in the aqueous medium by electro-Fenton oxidation.[10] Considering all oxidation reaction intermediates and products, a general reaction mechanism for ATZ degradation by OH was proposed. But the mechanism proposed in the experiment wasn't detailed enough. Mackul'ak identified the degradation products of atrazine by HPLC after application of the Fenton reaction and modified Fenton reaction, including some small organic molecules such as oxalic acid, urea, formic acid, acetic acid, and acetone. But their attention was focused on the small fragments of the degradation process that were identified by HPLC, the intermediates were not found.[41] Theoretical calculation can provide information for the reaction intermediates and pathways. Many theoretical studies on the degradation reaction by OH radical have been reported.[42,43] In this work, the density functional theory (DFT) calculation and the polarized continuum model (PCM)[44–46] were performed to investigate the degradation of ATZ by OH radical, and the roles of other components in Fenton's reagent have also considered. This study was helpful to further perfect the experimental mechanism, and could make up the inadequacy of experimental measurement on the short-lived substances, which provided the theoretical support for the removal of ATZ by Fenton oxidation treatment. In order to verify the theoretical results, liquid chromatography/mass spectrometry (LC/MS) analysis was used to identify the major intermediates and products.

Computational methods, experimental materials and analysis

Computational methods

Using the GAUSSIAN 09 programs,[47] high-level *ab initio* molecular orbital calculation is carried out for the reaction of ATZ with the OH radical. The geometrical parameters of stationary points are optimized at the M05-2X/6-31+G(d,p) level. The M05-2X functional is of high nonlocality with the double amount of nonlocal exchange (2×), which is an excellent method to predict noncovalent interactions.[48] The vibrational frequencies have been calculated at the same level in order to determine the nature of stationary points. Each transition state is verified to connect the designated reactants and products by performing an intrinsic reaction coordinate (IRC) analysis.[49] The PCM is chosen to calculate the solution-phase energy.

Materials and chemicals

Atrazine (ATZ > 98%) was purchased from Weifang Hua Yun Environmental Protection Technology Co., Ltd. Ferrous sulfate heptahydrate ($FeSO_4 \cdot 7H_2O$ >97%), hydrogen peroxide H_2O_2 (30%), HCl and sodium hydroxide NaOH were all analytical-grade and were purchased from Tianjin Kemiou Chemical Reagent Co., Ltd. All chemicals were used as being received without further purification.

Experiment methods

The stock solution of ATZ was prepared at 10 mg L^{-1} in distilled–deionized water, and the pH values of solutions were adjusted with HCl or NaOH. Two hundred milliliters of ATZ aqueous solution was added, adjusting pH prior to 2–3. The desired dosage of $FeSO_4 \cdot 7H_2O/H_2O_2$ was added thereafter to initiate the reaction. The mixture was magnetically stirred at 200 rpm at 25 °C. At different time intervals, 100 μL solution was taken out with an injector, and then filtered through 0.22 μm membranes before LC/MS analysis.

Experimental analysis

The oxidative degradation products of ATZ were analyzed by LC/MS with a LCQ Fleet (Thermo Fisher Scientific, USA), using a Waters SunFireTM-C18 column (4.6 mm × 250 mm, 5 μm). Electron spray ionization (ESI) was used with a spray voltage set at 5000 V; sheath gas flow rate, aux gas flow rate and capillary temperature were set at 30 arb, 10 arb, and 300 °C, respectively. The mass spectra data were obtained in the positive ion mode after scanning them from m/z 50 to 350.

Results and discussion

Initial reactions with OH radical

The OH radical addition to the C atom of triazine-ring, Cl atom substitution and H atom abstraction from ATZ are three possible kinds of channels for the reaction of ATZ with OH radical. The reaction pathways of OH radical addition, Cl atom substitution and H atom abstraction are depicted in Fig. 1 and 2, in which the potential barriers (E_a) and the reaction heats (E_r) are marked too. The optimized structures of the transition

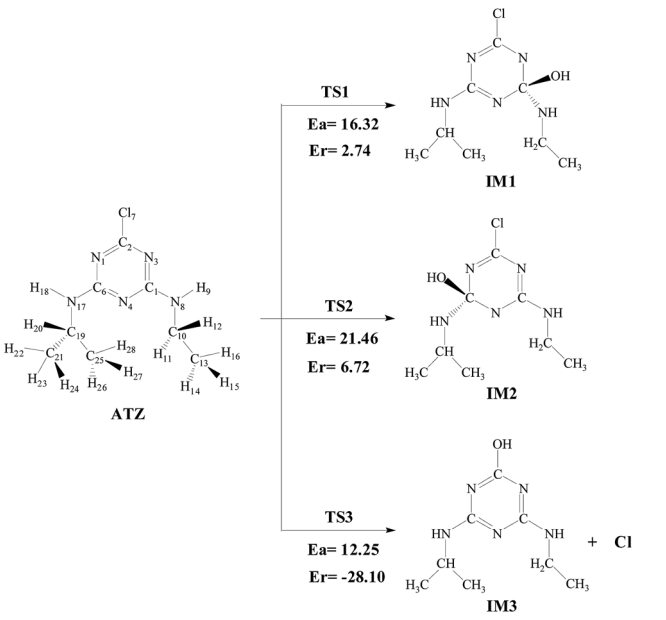

Fig. 1 OH radical addition pathways and Cl atom substitution pathway in aqueous solution with the potential barriers E_a (kcal mol^{-1}) and the reaction heats E_r (kcal mol^{-1}).

states involved in reactions of ATZ with OH radical are shown in Fig. 3.

A OH radical addition pathways. With the potential barriers of 16.32 and 21.46 kcal mol^{-1}, OH radicals are added to C_1 atom and C_3 atom in the triazine-ring, respectively. The lengths of the newly formed C_1–O bond and C_3–O bond in two transition-states are 1.768 and 1.774 Å, which are 0.380 and 0.382 Å longer than those in the corresponding ATZ-OH adducts. These processes are slightly endothermic, giving out 2.74 and 6.72 kcal mol^{-1} of energy, respectively. Thus, the ATZ-OH adducts are unstable, and can further react with the dissolved oxygen in water.

B Cl atom substitution pathway. Since OH is a strongly nucleophilic radical, the Cl atom which is attached to C_5 atom can be substituted for OH radical, producing hydroxyatrazine (HA, denoted as IM3) and Cl atom. This process crosses a potential barrier with 12.25 kcal mol^{-1} of energy, which is lower than the barrier added to the C_1 and C_3 atom of C=N bond. This reaction is strongly exothermic, releasing 28.10 kcal mol^{-1} of energy, implying that Cl atom substitution pathway is an energetically favorable reaction. HA is stable and has been detected in the experiment.[10]

C H atom abstraction pathways. As shown in Fig. 2, six H-abstraction sites exist in ATZ structure: two in the ethyl group, two in the iso-propyl group, one in the –NH– of ethylamino and one in the –NH– of iso-propylamino.

In the ethyl group, *i.e.*, $–CH_2CH_3$, the OH radical can abstract H atom from either $–CH_2–$ group or the $–CH_3$ group. A transition state (TS4) was found in the abstraction of H atom in $–CH_3$ group. This process has a potential barrier with 7.38 kcal mol^{-1} and is exothermic releasing 14.29 kcal mol^{-1} of energy. In H atom abstraction from the $–CH_2–$ group, OH radical abstracts H atom to produce IM5 *via* a small potential barrier with 2.02 kcal mol^{-1} of energy. This reaction is strongly exothermic, sending out 25.60 kcal mol^{-1} of energy, which shows that the H abstraction from the $–CH_2–$ group is easier than the H abstraction from the $–CH_3$ group.

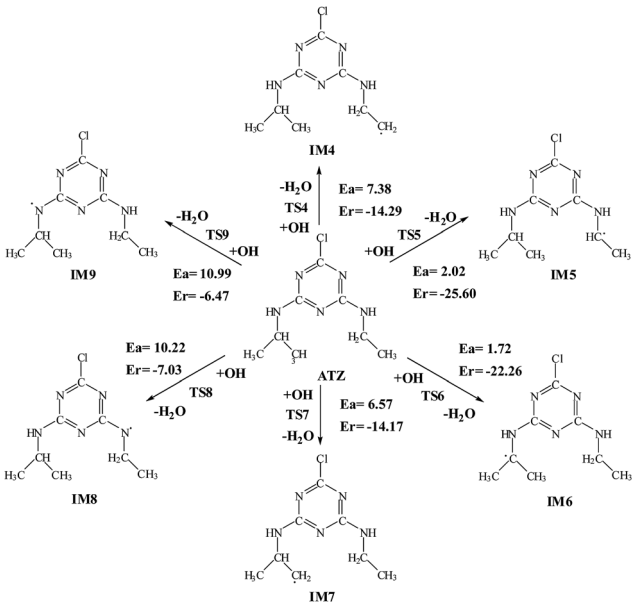

Fig. 2 H atom abstraction pathways in aqueous solution with the potential barriers E_a (kcal mol^{-1}) and the reaction heats E_r (kcal mol^{-1}).

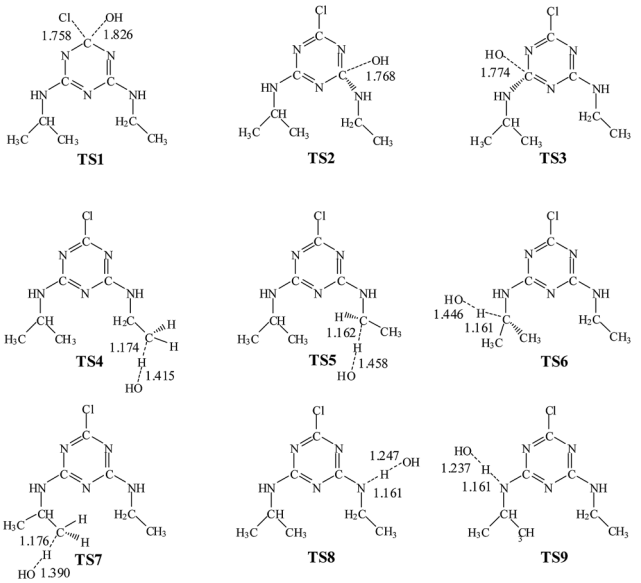

Fig. 3 Optimized geometries for the transition states involved in the initial reactions with OH radical. Distances are in angstroms.

H atom is abstracted from the iso-propyl group, *i.e.*, the $–CH(CH_3)_2$ group proceeds *via* either –CH– group or the $–CH_3$ group. These reactions are required to overcome the barrier with 1.72 and 6.57 kcal mol^{-1} of energy, and are strongly exothermic, releasing 22.26 and 14.17 kcal mol^{-1} of energy, respectively. Therefore, the abstraction from the –CH– group takes place more easily than H abstraction from the $–CH_3$ group.

As to H atom abstraction from the –NH– of ethylamino and –NH– of iso-propylamino, *i.e.*, $–NHCH_2CH_3$ and $–NHCH(CH_3)_2$, the two reactions need to cross the barrier of 10.22 and 10.99 kcal mol^{-1} and are exothermic, giving out 7.03 and 6.47 kcal mol^{-1} of energy, respectively. Comparison of these initial reactions with OH radicals show that H atom abstraction from the –CH– of $–CH(CH_3)_2$ group and the $–CH_2–$ of $–CH_2CH_3$ group can occur more easily and are expected to play an important role in further reactions. Therefore, the ethyl group is more reactive than the isopropyl group during OH radical attack, which is consistent with the research of Acero.[33]

Water catalysis in subsequent reactions

From the point of thermodynamics, H atom abstraction pathways are easier to take place than OH radical addition pathways and Cl atom substitution pathway. And H atom abstraction from the –CH– of $–CH(CH_3)_2$ group and the $–CH_2–$ group of $–CH_2CH_3$ are expected to occur more easily. Thus, in this section, intermediates IM5 and IM6 are selected as reactants in the following degradation process.

The production of carbon-centered radicals, IM5 and IM6, can be combined with OH radicals through barrierless reactions, generating IM10 and IM11. These processes are strongly

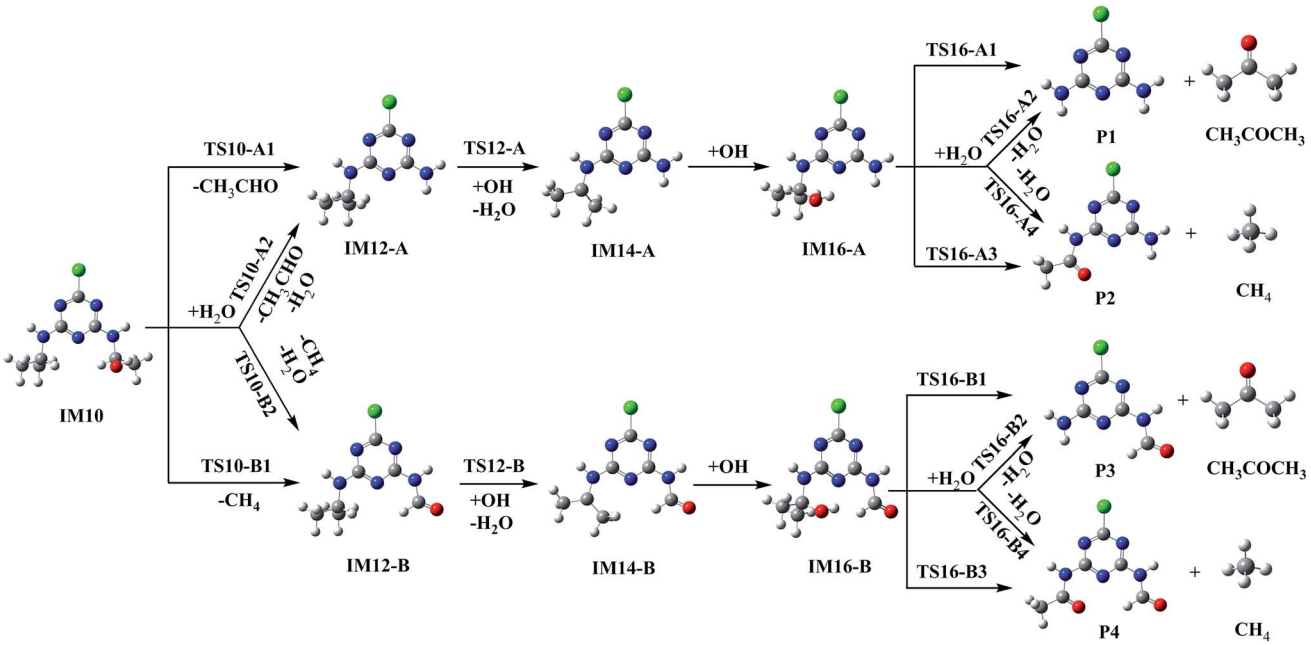

Fig. 4 The dealkylation and alkyl oxidation process of IM10 in aqueous medium by Fenton oxidation technology.

Table 1 The potential barriers (E_a) and reaction heats (E_r) of following reactions of IM10 and IM11

Reactions	Potential barriers (E_a)	Reaction heats (E_r)
IM10 → TS10-A1 → IM12-A + CH_3CHO	54.75	13.91
IM10 + H_2O → TS10-A2 → IM12-A + CH_3CHO + H_2O	25.22	13.91
IM12-A + OH → TS12A → IM14-A + H_2O	3.68	−20.66
IM14-A + OH → IM16-A	—	−96.84
IM16-A → TS16-A1 → P1 + CH_3COCH_3	54.47	8.28
IM16-A + H_2O → TS16-A2 → P1 + CH_3COCH_3 + H_2O	31.12	8.28
IM16-A → TS16-A3 → P2 + CH_4	84.03	7.65
IM16-A + H_2O → TS16-A4 → P2 + CH_4 + H_2O	66.79	7.65
IM10 → TS10-B1 → IM12-B + CH_3CHO	83.83	8.85
IM10 + H_2O → TS10-B2 → IM12-B + CH_3CHO + H_2O	59.99	8.85
IM12-B + OH → TS12B → IM14-B + H_2O	6.02	−21.04
IM14-B + OH → IM16-B	—	−94.92
IM16-B → TS16-B1 → P3 + CH_3COCH_3	54.65	7.11
IM16-B + H_2O → TS16-B2 → P3 + CH_3COCH_3 + H_2O	24.45	7.11
IM16-B → TS16-B3 → P4 + CH_4	84.56	7.84
IM16-B + H_2O → TS16-B4 → P4 + CH_4 + H_2O	64.10	7.84
IM11 → TS11-A1 → IM13-A + CH_3COCH_3	53.84	8.27
IM11 + H_2O → TS11-A2 → IM13-A + CH_3COCH_3 + H_2O	24.72	8.27
IM13-A + OH → TS3A → IM15-A + H_2O	3.20	−24.43
IM15-A + OH → IM17-A	—	−95.04
IM17-A → TS17-A1 → P1 + CH_3CHO	56.71	15.74
IM17-A + H_2O → TS17-A2 → P1 + CH_3CHO + H_2O	26.70	15.74
IM17-A → TS17-A3 → P3 + CH_4	83.11	11.07
IM17-A + H_2O → TS17-A4 → P3 + CH_4 + H_2O	60.27	11.07
IM11 → TS11-B1 → IM13-B + CH_3COCH_3	88.41	6.81
IM11 + H_2O → TS11-B2 → IM13-B + CH_3COCH_3 + H_2O	66.86	6.81
IM13-B + OH → TS3B → IM15-B + H_2O	4.64	−23.80
IM15-B + OH → IM17-B	—	−94.08
IM17-B → TS17-B1 → P2 + CH_3CHO	57.95	14.98
IM17-B + H_2O → TS17-B2 → P2 + CH_3CHO + H_2O	24.78	14.98
IM17-B → TS17-B3 → P4 + CH_4	82.38	11.66
IM17-B + H_2O → TS17-B4 → P4 + CH_4 + H_2O	59.55	11.66

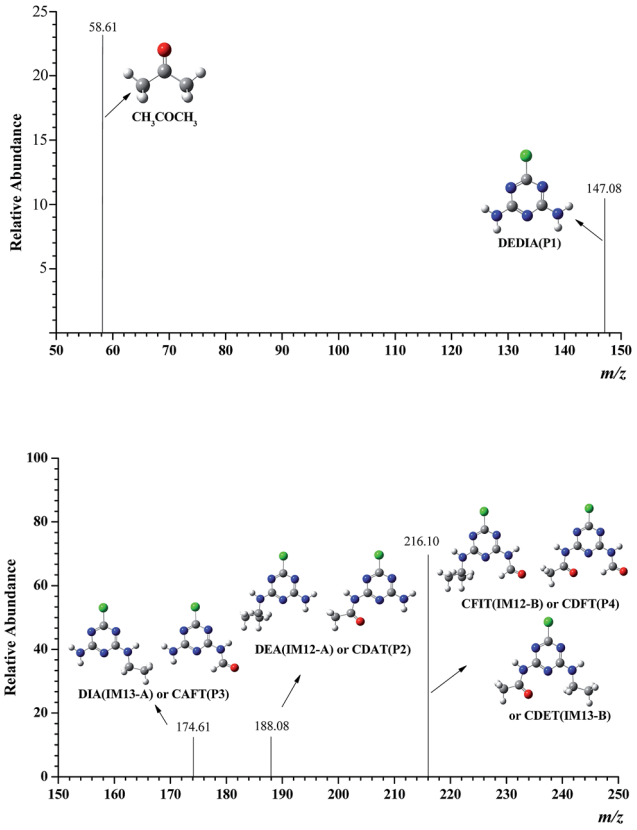

Fig. 5 The MS identification of ATZ degradation products.

endothermic, releasing 92.96 and 94.13 kcal mol^{-1} of energy. There are two ways in the following decomposition: dealkylation and alkyl oxidation with formation of formamide or acetamide. The reaction process is shown in Fig. 4 and S1.†

In the dealkylation reaction of IM10, the C_{10}–N_8 bond will be opened up, accompanied by the H atom migration from the O atom to the N_8 atom. The C_{10}–N_8 bond in the transition state TS10-A1 is elongated to 1.747 Å as shown in Fig. S2.† Deethylatrazine (DEA, denoted as IM12-A) and acetaldehyde (CH_3CHO) are produced *via* an apparent barrier of 54.75 kcal mol^{-1}, and this reaction is predicted to be endothermic, giving out 13.91 kcal mol^{-1} of energy. Given that the barrier of 54.75 kcal mol^{-1} is too high for this reaction to play an important role, we took into account the possible role of a H_2O. TS10-A2 shows that H_2O acts as a catalyst with one H atom moving to the N_8 atom simultaneously and extracting an H atom from the OH group. The C_{10}–N_8 bond will also be broken in this process *via* the barrier of 25.22 kcal mol^{-1}. This process is a concerted reaction. The water serves as a catalyst to reduce the reaction barrier dramatically. Although this activation barrier is still high, it is smaller compared to the energy released from the combination of IM5 and OH radical.

Besides the dealkylation, IM10 can also ignite alkyl oxidation reaction with formamide. With a high barrier of 83.83 kcal mol^{-1}, the C_{10}–C_{13} bond will be broken along with the H migration from O to C_{13} *via* a transition state TS10-B1 (Fig. 4). 2-Chloro-4-formamido-6-isopropylamin-*s*-triazine (CFIT, denoted as IM12-B) and methane (CH_4) will be produced in this reaction. When H_2O gets involved in the reaction, it will act as a catalyst and reduce the barrier to 59.99 kcal mol^{-1} as shown in Fig. 4 and Table 1.

Then in IM12-A and IM12-B, dealkylation or alkyl oxidation can occur with three steps including H atom abstraction forming IM14-A and IM14-B, OH radical barrierless addition forming IM16-A and IM16-B, and C–N bond or C–C bond cleavage along with H atom migration. Then the stable products, deethyldeisopropylatrazine (DEDIA, denoted as P1), 6-acetamido-4-amino-2-chloro-*s*-triazine (CDAT, denoted as P2), 6-amino-2-chloro-4-formamido-*s*-triazine (CAFT, denoted as P3), 6-acetamido-2-chloro-4-formamido-*s*-triazine (CDFT, denoted as P4), acetone (CH_3COCH_3) and CH_4 can come into being.

The decomposition of IM11 has undergone the similar pathways, and the schematic diagram of the reaction pathways and the optimized geometries for the transition states are drawn in Fig. S1 and S2,† respectively. However, it is worth noting that deisopropylatrazine (DIA, denoted as IM13-A) and 6-acetamido-2-chloro-4-ethylamino-*s*-triazine (CDET, denoted as IM13-B) will be formed.

The identification of degradation products

The degradation products of the ATZ were identified by LC/MS analysis and listed in Fig. 5. Several products had prominent protonated molecular ion at *m*/*z* 58.61, 147.08, 174.61, 188.08, 216.10, which were preliminarily identified as CH_3COCH_3, DEDIA(P1), DIA(IM13-A) or CAFT(P3), DEA(IM12-A) or CDAT(P2), CFIT(IM12-B) or CDFT(P4) or CDET(IM13-B). Products DEDIA, DIA, DEA, CDAT and CDET had been found out in earlier studies.[10,33] Others were observed for the first time in the Fenton system.

The toxicity of ATZ and its degradation products have been evaluated in several studies. Ralston-Hooper *et al.* evaluated the acute and chronic toxicity in the amphipods *Hyalella azteca* and *Diporeia* spp., and in the unicellular algae *Pseudokirchneriella subcapitata*, and they concluded that acute and chronic toxicities were ranked ATZ > DEA > DIA.[50] Tchounwouli compared the toxicities of ATZ, DEA, DIA and DEDIA by Microtox Assay. They found that DEA and DIA are the least toxic, with EC50 81.86 and 82.68 mg L^{-1}, followed by ATZ (EC_{50} = 39.87 mg L^{-1}), which is consistent with the former.[51] The EC_{50} of DEDIA is 12.74 mg L^{-1}, and it suggests that the final product has more toxicity than that of ATZ.

Conclusions

The new degradation mechanism of ATZ in aqueous solutions has been investigated. From the point of thermodynamics, H atom abstraction pathways are easier to take place than those of OH radical addition and Cl atom substitution. Moreover, H atom abstraction from –CH– of $–CH(CH_3)_2$ group and $–CH_2–$ group of $–CH_2CH_3$ are the main OH-initiated reactions of ATZ.

The subsequent decomposition of IM10 and IM11 involves two ways: dealkylation and alkyl oxidation with formation of

formamide or acetamide. It should be pointed out that H_2O can act as a catalyst to reduce the reaction barrier in these processes dramatically which is helpful to interpret the high efficiency of Fenton reagents. This mechanism can also provide a new point for the OH-initiated chemical transformation of volatile organic compounds in atmosphere.

The stable intermediates and products, CH_3COCH_3, DEDIA, DIA, DEA, CAFT, CDAT, CDET, CDFT and CFIT, have been observed experimentally. This study offers a cost-effective way to probe the degradation mechanism of ATZ in the aqueous medium by Fenton oxidation technology.

Acknowledgements

This work is supported by National Natural Science Foundation of China (21277082, 21337001, 21607011, 21577021, 21377028, 21177025), Natural Science Foundation of Shandong Province (No. ZR2014BP012), Program for New Century Excellent Talents in University (NCET-13-0349), Project for science and technology development of Shandong province (2014GSF117028), Beijing National Laboratory for Molecular Science (20140160), and the Fundamental Research Funds of Shandong University (2015JC020).

Notes and references

1 D. Barcelo, *Analyst*, 1991, **116**, 681–689.
2 R. I. Bonansea, M. V. Ame and D. A. Wunderlin, *Chemosphere*, 2013, **90**, 1860–1869.
3 M. L. M. Tagert, J. H. Massey and D. R. Shaw, *Sci. Total Environ.*, 2014, **481**, 564–573.
4 K. B. Delwiche, J. Lehmann and M. T. Walter, *Chemosphere*, 2014, **95**, 346–352.
5 D. C. Reid, A. C. Dwards, D. Cooper, E. Wilson and B. A. Mcgaw, *Water Res.*, 2003, **37**, 245–254.
6 G. D. Cimino-Reale, F. B. Casati, R. Brustio, C. Diodovich, A. Collotta, M. Vahter and L. Gribaldo, *Toxicol. Lett.*, 2008, **180**, 59–66.
7 M. Kucka, K. Pogrmic-Majkic, S. Fa, S. S. Stojilkovic and R. Kovacevic, *Toxicol. Appl. Pharmacol.*, 2012, **265**, 19–26.
8 S. O. Abarikwu, E. O. Farombi and A. B. Pant, *Toxicol. Lett.*, 2013, **221**, S215.
9 S. R. Muller, M. Berg, M. M. Ulrich and R. P. Schwarzenbach, *Environ. Sci. Technol.*, 1997, **31**, 2104–2113.
10 B. Balci, N. Oturan, R. Cherrier and M. A. Oturan, *Water Res.*, 2009, **43**, 1924–1934.
11 K. H. Chan and W. Chu, *Chemosphere*, 2003, **51**, 305–311.
12 C. D. Adams and T. L. Watson, *J. Environ. Eng.*, 1996, **122**, 327–330.
13 P. Ghosh, L. Philip and M. Bandyopadhyay, *Pract. Period. Hazard., Toxic, Radioact. Waste Manage.*, 2005, **9**, 112–121.
14 A. Yassir, B. Lagacherie, S. Houot and G. Soulas, *Pestic. Sci.*, 1999, **55**, 799–809.
15 C. B. Shaw, C. M. Carliell and A. D. Wheately, *Water Res.*, 2002, **36**, 1193–2001.
16 L. P. Wackett, M. J. Sadowsky, B. Martinez and N. Shapir, *Appl. Microbiol. Biotechnol.*, 2002, **58**, 39–45.
17 J. Marugán, J. Aguado, W. Gernjak and S. Malato, *Catal. Today*, 2007, **129**, 59–68.
18 H. L. Chen, E. Bramanti, I. Longo, M. Onor and C. Ferrari, *J. Hazard. Mater.*, 2011, **186**, 1808–1815.
19 K. H. Chan and W. Chu, *Appl. Catal., B*, 2005, **58**, 157–163.
20 K. H. Chan and W. Chu, *Water Res.*, 2003, **37**, 3997–4003.
21 D. H. Belhateche, *Chem. Eng. Prog.*, 1995, **91**, 32–51.
22 C. D. Adams and S. J. Randtke, *Environ. Sci. Technol.*, 1992, **26**, 2218–2227.
23 L. P. Wackett, M. J. Sadowsky, B. Martinez and N. Shapir, *Appl. Microbiol. Biotechnol.*, 2002, **58**, 39–45.
24 C. Petrier, B. David and S. Laguian, *Chemosphere*, 1996, **32**, 1709–1718.
25 A. Hiskia, M. Ecke, A. Troupis, A. Kokorakis, H. Hennig and E. Papaconstantinou, *Environ. Sci. Technol.*, 2001, **35**, 2358–2364.
26 G. Xu, J. Z. Yao, L. Tang, X. Y. Yang, M. Zheng, H. Wang and M. H. Wu, *Chem. Eng. J.*, 2015, **275**, 374–380.
27 O. Sacco, V. Vaiano, C. Han, D. Sannino and D. D. Dionysiou, *Appl. Catal., B*, 2015, **164**, 462–474.
28 J. A. Santacruz-Chávez, S. Oros-Ruiz, B. Prado and R. J. Zanella, *J. Environ. Chem. Eng.*, 2015, **3**, 3055–3061.
29 S. Nelieu, L. Kerhoas and J. Einhorn, *Environ. Sci. Technol.*, 2000, **34**, 430–437.
30 R. C. L. Silva, R. J. Carvalho and B. A. Calfa, *Rev. Ambiente Agua*, 2010, **5**, 9–20.
31 G. Y. S. Chan, J. M. Hudson and N. S. J. Isaacs, *Phys. Org. Chem.*, 1992, **5**, 600–608.
32 C. W. Luo, J. Ma, J. Jiang, Y. Z. Liu, Y. Song, Y. Yang, Y. H. Guan and D. J. Wu, *Water Res.*, 2015, **80**, 99–108.
33 J. L. Acero, K. Stemmler and U. Von Gunten, *Environ. Sci. Technol.*, 2000, **34**, 591–597.
34 S. M. Arnold, W. J. Hickey and R. F. Harris, *Environ. Sci. Technol.*, 1995, **29**, 2083–2089.
35 J. De Laat, H. Gallard, A. Ancelin and B. Legube, *Chemosphere*, 1999, **39**, 2693–2706.
36 P. L. Huston and J. J. Pignatello, *Water Res.*, 1999, **33**, 1238–1246.
37 K. Pratap and A. T. Lemley, *J. Agric. Food Chem.*, 1998, **46**, 3285–3291.
38 A. Ventura, G. Jacquet, A. Bermond and V. Camel, *Water Res.*, 2002, **36**, 3517–3522.
39 J. C. Barreiro, M. D. Capelato, L. Martin-Neto and H. C. B. Hansen, *Water Res.*, 2007, **41**, 55–62.
40 J. A. Khan, X. He, H. M. Khan, N. S. Shah and D. D. Dionysiou, *Chem. Eng. J.*, 2013, **218**, 376–383.
41 T. Mackul'ak, J. Prousek and L. '. Švorc, *Monatsh. Chem.*, 2011, **142**, 561–567.
42 Q. Z. Zhang, X. H. Qu and W. X. Wang, *Environ. Sci. Technol.*, 2007, **41**, 6109–6116.
43 X. M. Sun, T. L. Sun, Q. Z. Zhang and W. X. Wang, *Sci. Total Environ.*, 2008, **402**, 123–129.
44 V. Barone and M. Cossi, *J. Phys. Chem. A*, 1998, **102**, 1995–2001.
45 V. Barone, M. Cossi and J. Tomasi, *J. Comput. Chem.*, 1998, **19**, 404–417.

46 B. Mennucci and J. Tomasi, *J. Chem. Phys.*, 1996, **106**, 5151–5158.
47 M. J. Frisch, G. W. Trucks, H. B. Schlegel and G. E. Scuseria, *et al.*, *Gaussian 09, revision D.01*, Gaussian, Inc., Wallingford, CT, 2009.
48 Y. Zhao, N. E. Schultz and D. G. Truhlar, *J. Chem. Theory Comput.*, 2006, **2**, 364–382.
49 K. Fukui, *Acc. Chem. Res.*, 1981, **14**, 363–368.
50 K. Ralston-Hooper, J. Hardy, L. Hahn, H. Ochoa-Acuna, L. S. Lee, R. Mollenhauer and M. S. Sepúlveda, *Ecotoxicology*, 2009, **18**, 899–905.
51 P. B. Tchounwouli, B. Wilson, A. Ishaque, R. Ransome, M. J. Huang and J. Leszczynski, *Int. J. Mol. Sci.*, 2000, **1**, 63–74.